Designing a Multifunctional Chromatography Stationary Phase for (Bio)Product Purification via Green Chemistry

LUNDS UNIVERSITET

Author: Xiaolin Lei

Supervisor: Solmaz Hajizadeh

Examiner: Lei Ye

Degree project in MSc Biochemistry Programme

Department of Pure and Applied Biochemistry

Lund University, 2024

Abstract

The multifunctional cryogels were synthesized by atom transfer radical polymerization (ATRP) using hemoglobin as a biocatalyst (ATRPase) and post-modified to purify hemoglobin and glycoprotein simultaneously. Meanwhile, the optimization of purified glycoprotein was also conducted by introducing epoxy group nanoparticles. The nanoparticle concentrated concanavalin A, the ligand, to adsorb glycoprotein effectively. Scanning electron microscopy (SEM) was used to characterize the morphology of cryogels with/without nanoparticles. Batch adsorption and kinetics adsorption were used to evaluate the adsorption capacity and behavior of the chromatography columns. The Langmuir and bis-Langmuir models were used to fit the batch adsorption of glycoprotein and hemoglobin, respectively. For kinetics adsorption, both proteins were followed by the pseudo-second-order model. Based on these models, the theoretical maximum capacity was calculated and compared. The maximum capacity of hemoglobin was 148.58 and 309.70 mg protein/mL cryogels for cryogels with/without nanoparticles; The maximum capacity of ovalbumin, a glycoprotein, was 93.98 and 43.63 mg protein/mL cryogels for cryogels with/without nanoparticles. It was found that introducing nanoparticles can enhance the efficiency of glycoprotein purification by increasing the concentration of immobilized ligands, which increased 50.35 mg protein/mL cryogels. However, immobilizing nanoparticles impacted hemoglobin adsorption and reduced it.

Contents

1. Introduction

The rapid advancement of the biotechnology industry significantly contributes to society. It has a wide range of applications, such as biofuels, pharmaceuticals, and biotherapeutic materials (Gao et al., 2020). There is also a growing demand for high-purity bioproducts. Thus, obtaining high-quality bioproducts more efficiently and at lower costs is essential. Recent decades have seen remarkable technological improvements in upstream processes, which caused significant increases in bioproduct yield. The increase of recombinant protein yield for various monoclonal antibodies went from tens of milligrams per liter in cell culture to as much as 10 grams per liter (Wurm, 2004). As the production scale increased, downstream processing limitations emerged (Gottschalk, 2008). Thus, optimizing the downstream process is crucial to save time and cost. The significant point is to select the appropriate separation and purification technique, such as extraction, filtration, chromatography, etc.

Chromatography is widely applied to protein purification, especially affinity chromatography. As an essential step in the downstream process, improving the purification efficiency of chromatography is highly valuable in optimizing the downstream process. The interaction between the substances contained in the mixture and the stationary phase is crucial in the chromatography purification process (Coşkun, 2016). Designing the multifunctional stationary phase can separate multiple proteins in a single step, significantly enhancing purification efficiency and saving time.

The characteristic of the stationary phase forms the basis of the chromatographic system, which decides the performance of the separation of chromatography. Hydrogels are gels with water acting as a swelling agent and a hydrophilic polymer as the network component, which may contain various functional groups and possess properties such as excellent biocompatibility and robust adhesion, making them ideal candidates for chromatographic stationary phases (Zhang et al., 2023). Cryogels are a category of hydrogels that have macropores and elastic interconnected networks. It is formed through cryogelation polymerization at sub-zero temperatures (Memić et al., 2019). Cryogels, as a polymeric material, have wide applications in bioseparation, tissue engineering, drug delivery, food technology, and so on (Baimenov et al., 2020).

Due to ice crystal formation in cryogel formation, porous structures are generated. Super macroporous causes intricate substances like raw extracts, cellular material, and blood to pass cryogels without pretreatment. This can shorten the downstream process by eliminating clarification steps such as filtration and centrifugation. Thus, time and cost are also reduced by decreasing the number of unit operations in the downstream process (Solmaz, 2023). Therefore, cryogels are highly effective in purifying proteins, which can be used as chromatography's stationary phase in bioseparation.

Radical polymerization is the most widely used industrial method since it is suitable for various vinyl monomers, has flexible reaction conditions (requiring merely the removal of oxygen), and tolerates water and impurities (Coessens et al., 2001). However, the polymer structure is not under its control, leading to high molecular weight and polydispersity. Ionic polymerization produces precisely structured polymers with regulated end functionalities. and block copolymers but requires a strictly moisture-free environment and very low temperatures. It is limited to a few monomers and can have unexpected side reactions due to functional groups in the monomers (Coessens et al., 2001). In this project, a chosen polymerization method to form cryogels is atom transfer radical polymerization (ATRP). ATRP is a controlled radical method, forming polymers with well-defined

molecular weights and end functionalities, which are decided by the ratio of monomer consumed to the initiator. This method is achieved using transition metals as catalysts. ATRP offers several advantages: it generates well-defined polymers with low polydispersity and permits the polymerization of various monomers. It enables the creation of polymers with diverse structures and precise end group control, allowing for easy incorporation of specific functionalities. This versatility makes ATRP ideal for creating polymers with tailored properties for advanced applications. (Coessens et al., 2001). Effectively removing the catalyst remains a primary challenge in commercializing the ATRP process (Matyjaszewski & Xia, 2001). Instead of using metals as ATRP catalysts, biocatalysts such as metalloproteins can also be utilized, where the reaction is known as ATRPase (Kali et al., 2012). In this project, hemoglobin as the biocatalyst was applied to synthesize cryogels. To the author's knowledge, it is the first time ATRPase has been carried out under frozen conditions, which will be explored in this project.

Another technique that was used in this thesis and merged with ATRP and cryogelation polymerization is molecular imprinting. Molecularly imprinted polymer (MIP) is a synthetic polymer formed by this technique, which provides several benefits. They have high affinity and selectivity comparable to biological receptors, reusability, easy engineering, and low production costs. These attributes make MIPs highly applicable in numerous fields, such as immunoassays, affinity separation, cell and tissue imaging, drug delivery, and so on (Beyazit et al., 2016).

This project focuses on designing multifunctional cryogels as the stationary phase of chromatography to improve purification efficiency. No additional catalyst is required in the polymerization system because hemoglobin was used as a biocatalyst for the ATRPase reaction as well as the template for molecular imprinting. Their ATRPase activity is a helpful tool for synthetic polymer chemistry, and hemoglobin is easily accessible, safe for the environment, and non-toxic. Additionally, the comprehension of hemoglobin's redox chemistry is improved by this new activity (Silva et al., 2013). The basic principle is that the hemoglobin as the template forms covalent or non-covalent bonds with functional monomers. The polymerization is conducted under the influence of a crosslinker; after polymerization is completed, the template, hemoglobin, is washed off and removed from the network. Thus, the specific binding sites or empty cavities are generated on the surface of the gel, which match the size and shape of hemoglobin (He et al., 2021).

Synthesized cryogels were modified with a second ligand, concanavalin A (Con A), to capture glycoprotein (Bercea & Lupu, 2024). Therefore, cryogels can purify hemoglobin and glycoprotein at the same time. Immobilization of Con A was done after cryogelation by introducing epoxy groups to the surface of the cryogel and then covalently binding the ligands to epoxy pendants. To optimize the purification efficiency of glycoprotein, epoxy nanoparticles were introduced to this system to increase the number of ligands and compare the adsorption behavior with cryogels without nanoparticles. The maximum capacity is a significant standard to evaluate the adsorption of cryogels. In this project, ovalbumin is selected to represent glycoproteins.

2. Materials and Methods

2.1 Materials

Acrylamide (AAm), *N*-(3-aminopropyl)methacrylamide (APMA), *N,N′*-methylene-bis-acrylamide (mBAAm), *N,N*-dimethyl-*N′*-ethylethylenediamine 99% (TEMED), 2-hydroxyethyl 2-bromoisobutyrate (HEBIB), concanavalin A (Con A), acetic acid, sodium dodecyl sulfate (SDS), sodium carbonate, sodium hydrogen carbonate, sodium dihydrogen phosphate, sodium hydrogen phosphate, fructose, bovine serum albumin (BSA), hemoglobin (Hb), ovalbumin (OVA), 4-20% stain-free precast gels, sodium hydroxide, sodium chloride (obtained from Aldrich in Steinheim, Germany), calcium chloride, magnesium chloride (purchased by Merck in Darmstadt, Germany).

2.2 Synthesis of Cryogels

Cryogels were inspired to be prepared by atom transfer radical polymerization (Matyjaszewski & Xia, 2001). AAm and APMA were used as monomers, and mBAAm was used as a crosslinker. Appropriate amounts of monomers, based on **Table 1**, were dissolved in 4 ml water. Then, TEMED and HEBIB were added to the solution, which stirred in ice. The soluble oxygen in the solution was removed by degassing for 15 minutes under vacuum. Hemoglobin and ascorbic acid were dissolved separately in water and degassed under vacuum for 1 hour and 10 minutes, respectively. Five mL hemoglobin solution and 1 mL ascorbic acid solution were transferred to monomers solution and then degassed for 5 minutes. 0.5 mL of the final mixture was transferred into pre-cooled glass tubes (i.d. 1 cm) sealed from the top and bottom to limit oxygen access. Subsequently, the sealed tubes were placed in a cryostat and kept for seven days at -12 °C. The frozen samples were thawed at room temperature and then washed three to five times with distilled water.

Two different washing approaches were used to remove the hemoglobin: a) for cryogels with nanoparticles, the gels were washed with 10% acetic acid containing 1% SDS overnight, then rinsed with water until the pH became neutral. Finally, the 0.1 M sodium carbonate buffer was used to wash these cryogels for 1 hour. b) For cryogels without nanoparticles, the gels were washed with 0.1 M sodium hydroxide for 1 hour. Then, gels were incubated in 0.5 M sodium hydroxide containing epichlorohydrin (2% v/v) to introduce epoxy groups at 40 ℃ for 24 hours. Next, these cryogels were rinsed with water until the pH became neutral. All the gels were kept and dried in an oven overnight at 60 °C.

Table 1. The amounts of chemicals involved in the synthesis of cryogels

AAm (g)	APMA (g)	mBAAm (g)	TEMED (μL)	HEBIB (μL)	Hemoglobin (mg)	Ascorbic acid (mg)	Water (mL)
0.36	0.14	0.10	10	10	140	30	10

2.3 Ligand immobilization

2.3.1 Ligands immobilized on cryogels directly

Con A (60 mg) was dissolved in 50 mM sodium carbonate buffer containing 1 M NaCl, 1 mM $CaCl_2$, 1 mM $MgCl_2$ (30 mL). Dried cryogels with epoxy groups were added to tubes with 2 mL Con A solution and placed on the rocking table for 24 hours at room temperature. The gels were washed with the buffer and then incubated in 0.1 M ethanolamine in the same buffer to block the non-reacted epoxy group.

2.3.2 Ligands immobilized on cryogels with epoxy nanoparticles

Epoxy nanoparticles were organic nanoparticles synthesized by methyl methacrylate (MMA) and glycidyl methacrylate (GMA), as mentioned elsewhere (Hajizadeh et al., 2013). The diameter of the epoxy nanoparticles was about 1000 nm in an aqueous solution measured by dynamic Light Scattering (DLS) (Zetasizer Nano ZS, Malverm Instruments, UK).

Epoxy nanoparticles were dispersed in 0.1 M sodium carbonate buffer. The particle suspension was circulated through the cryogel with active amine groups on its surface using a peristaltic pump (flow rate 2 mL/min) for 8 hours. The cryogel was washed using 0.1 M sodium carbonate buffer overnight to remove non-reacted epoxy nanoparticles. The immobilization procedure of Con A was followed as described in 2.3.1.

2.4 Characterization of cryogels

Polymerization yield for cryogels was calculated using **Equation 1**. m_0 is theoretical weight and m_1 is the dried weight of cryogels.

$$Y = \frac{m_1}{m_0} \qquad \textbf{Equation 1}$$

The swelling ratio is another standard to characterize cryogels' properties, which can be calculated by **Equation 2**. m_2 is the mass of cryogels adsorbed water, m_3 is the mass of dried cryogels.

$$S = \frac{m_2 - m_3}{m_3} \qquad \textbf{Equation 2}$$

Scanning electron microscopy (SEM) (Hitachi SU3500, Hitachi, Japan) operated at 10 kV, which was used to characterize the morphology of cryogels.

Hemoglobin (7.5 mg) was dissolved in 15 ml PBS buffer. Then, gradient dilution was used to obtain different concentrations of hemoglobin solution: 0.5 mg/ml, 0.4 mg/ml, 0.3 mg/ml, 0.2 mg/ml,0.1 mg/ml, and 0.05 mg/ml. The adsorption of these protein solutions was read at 405 nm wavelength by UV/Vis spectrometer. Based on the reading and concentration, the calibration curve and equation of hemoglobin can be obtained.

Ovalbumin (30 mg) was dissolved in 15 ml PBS buffer. Then, gradient dilution was used to obtain

different concentrations of ovalbumin solution: 2 mg/ml, 1.5 mg/ml, 1 mg/ml, 0.5 mg/ml, and 0.3 mg/ml. The adsorption of these protein solutions was read at 280 nm wavelength by the spectrometer. Based on the reading and concentration, the calibration curve and equation of ovalbumin can be obtained.

2.5 Batch Adsorption

Hemoglobin (60 mg) was dissolved in 15 ml PBS buffer. Then, gradient dilution was used to obtain different concentrations of hemoglobin solution: 4 mg/ml, 3 mg/ml, 2 mg/ml, 1.5 mg/ml,1 mg/ml, 0.5 mg/ml, 0.3 mg/ml, and 0.1 mg/ml. Cryogels were added to each tube and placed on the rocking table in a cold room for 24 hours. The absorption of the initial and remaining solutions after adsorption were read at 405 nm wavelength by the spectrometer. By subtracting the remaining concentration in the solution from the initial concentration, the concentration of the protein adsorbed by the cryogel was calculated.

Ovalbumin (75 mg) was dissolved in 15 ml PBS buffer. Gradient dilution was used to obtain different concentrations of ovalbumin solution: 5 mg/ml, 4 mg/ml, 3 mg/ml, 2.5 mg/ml, 2 mg/ml,1.5 mg/ml, and 1 mg/ml. Then, cryogels were added to each tube and placed on the rocking table in a cold room for 24 hours. The amount of adsorbed ovalbumin on the cryogel was calculated as mentioned above, except that 280 nm was selected as the wavelength.

2.6 Kinetics Adsorption

Hemoglobin (90 mg) was dissolved in 30 mL PBS buffer, 2 mL of the 3 mg/ml protein solution, and cryogels were added to each tube. Then, the absorbance of 1, 2, 5, 10, 20, 30, 60, 120, 180, 240, 300, 360, 420, 480, and 1440 minutes were read at 405 nm wavelength by spectrometer. The adsorbed amount on the gel was done indirectly, as mentioned in section 2.5.

Ovalbumin (90 mg) was dissolved in 30 mL PBS buffer, 2 mL of the 3 mg/ml protein solution, and cryogels were added to each tube. Then, the absorbance of 1, 2, 5, 10, 20, 30, 60, 120, 180, 240, 300, 360, 420, 480, and 1440 minutes was read at 280 nm wavelength by the spectrometer, and the adsorbed amount on the gel was measured as mentioned earlier.

2.7 Selective Adsorption

To determine whether cryogels have selective adsorption to hemoglobin, the SDS-PAGE was used to detect protein types in different stage solutions. BSA (6 mg/ml) and Hemoglobin (3 mg/ml) were dissolved in 2 ml PBS buffer (a total of 3 different tubes). The cryogel with immobilized epoxy nanoparticles was added to each tube. Then, the reaction tube was placed on the rocking table in a cold room for 24 hours to adsorb the target protein. The loaded and eluted fractions were collected and detected in a spectrophotometer at 405 nm wavelength.

After 24 hours, the PBS buffer was used to wash cryogels. PBS buffer (2 mL) was added to each tube and washed for 3 hours in the cold room to remove non-specific binding protein. Similarly, wash fraction was collected and detected. The loaded, washed, and eluted fractions were freeze-dried to concentrate their protein. The samples were prepared for the SDS-PAGE procedure. Laemmli sample buffer was mixed with the protein solution at a 1:1 ratio and then boiled at 100°C

for 10 minutes. 12 μL of each sample was loaded into each well. The 100 V voltage was applied to the SDS-PAGE gel and ran for 1.5 hours. The gel was stained for 1 hour with a 0.25% Coomassie Brilliant (with acetic acid, methanol, and water) in gentle stirring conditions at room temperature. Next, the gel was destained overnight using a destained solution (with acetic acid, methanol, and water).

3. Results and discussion

3.1 Synthesis and modification of cryogels

3.1.1 Synthesis of Cryogels

The multifunctional cryogels can purify hemoglobin due to cavities formed by MIP and glycoprotein due to immobilized ligand, Con A. In this project, the synthesis of cryogels is an important part. AAm and APMA as the functional monomers and mBAAm as the crosslinker was used to synthesize the cryogels in a frozen state (-12℃). Hemoglobin acts as the biocatalyst in ATRPase reaction to form a polymeric network (Hajizadeh, Bülow, et al., 2021). The schematic image of the ATRPase polymerization is shown in **Figure 1**.

In addition, molecular imprinting was combined with cryogels synthesis. Hemoglobin also acts as a template for synthesizing composite cryogels to form MIP cavities. Thus, cryogels can be used to purify hemoglobin. Further modifications are needed to obtain more functionalities for the synthesized cryogels.

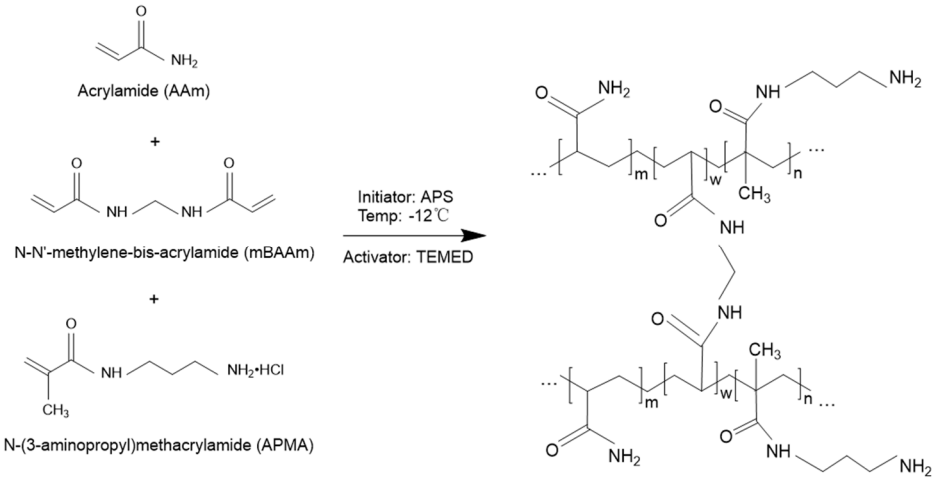

Figure 1. Scheme for the polymerization reaction during cryogels synthesis from three monomers (AAm, mBAAm, and APMA) and initiating system (initiator: HEBIB; activator: TEMED)

3.1.2 Modification of Cryogels

Con A is a lectin that can bind to glycoproteins through non-covalent interactions (Saleemuddin & Husain, 1991), which includes four specific binding sites with sugar. It has a high affinity to glycoprotein (Bercea & Lupu, 2024). Thus, this project used Con A as a ligand to capture glycoproteins. The cryogels were divided into two groups to have different modifications. The first group was to immobilize ligands directly on the surface of the cryogel via the available amine group in APMA building blocks. The amine groups were converted to the epoxy groups using epichlorohydrin. Then, the Con A ligands were attached to the cryogels covalently via epoxy groups. In the second group, organic nanoparticles containing free epoxy groups were immobilized on the surface of the cryogel to increase the number of immobilized ligands and, subsequently, the efficiency of glycoprotein separation. The difference between the groups is that the concentration of ligands is improved by introducing nanoparticles, which can improve the efficiency of glycoprotein purification.

The epoxy group nanoparticles were synthesized by methyl methacrylate 99% (MMA) and Glycidyl methacrylate (GMA) (Hajizadeh et al., 2013c). The synthesized nanoparticles were directly applied to this project as they were received. Dynamic Light Scattering (DLS) was used to represent the diameter of nanoparticles (**Figure 2**). The diameter of the nanoparticles ranges between 893.8 nm and 1039 nm. The polydispersity is 0.2292. Fourier Transform Infrared Spectroscopy (FTIR) (Nicolet iS5, Thermo Fisher Scientific Inc., Waltham, USA) was used to characterize epoxy groups. The epoxy group has absorption peaks at 831-915 cm^{-1} and was observed on the FTIR spectra of nanoparticles (**Figure 3**) (González et al., 2012).

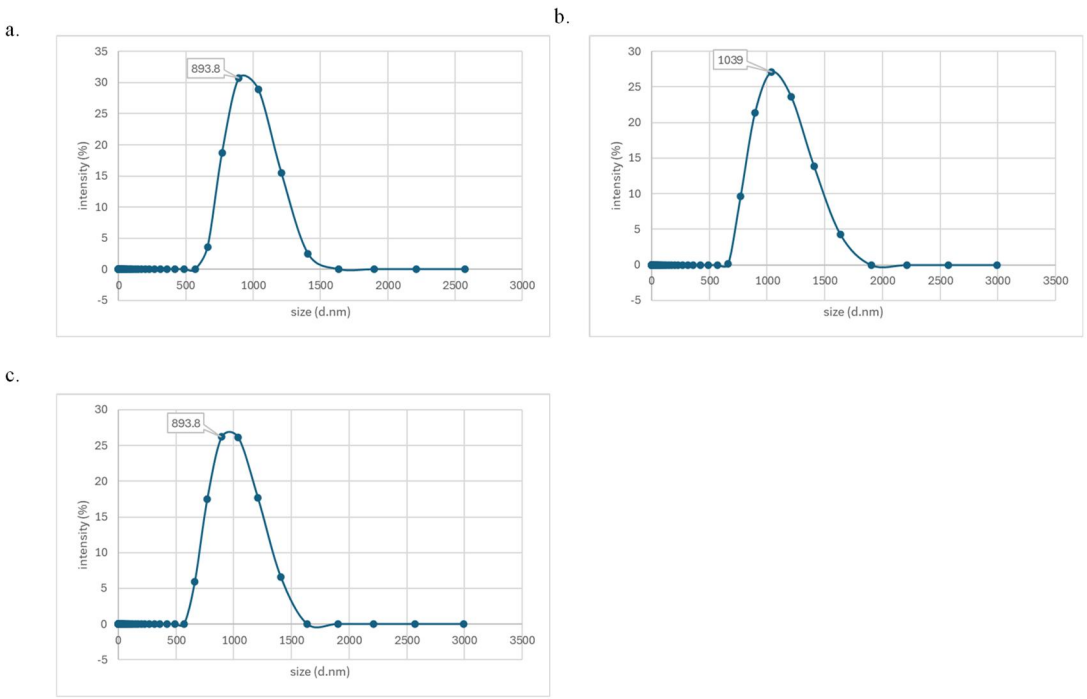

Figure 2. Three replicates of DLS intensity distribution graphs for epoxy group nanoparticles

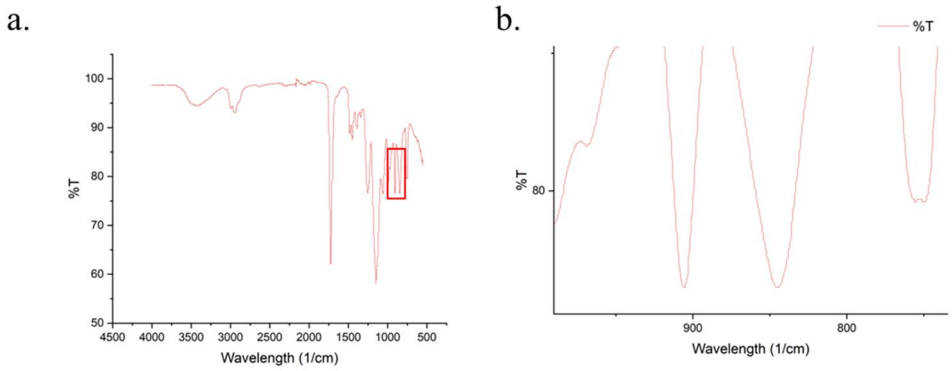

Figure 3. a) FTIR spectra of epoxy groups nanoparticles. b) a higher resolution of the image a.

3.2 Characterization of cryogels

Characterizing the structure of cryogels is essential for further exploration. In this section, polymerization yield and swelling ratio were necessary to evaluate the production and quality of cryogels. The swelling ratio represents the ability of cryogels to absorb water or other solutions and their swelling behavior when in contact with liquid (**Table 2**). Compared to radical polymerization, cryogels obtained via ATRPase show lower yields and swelling ratio (Trinh et al., 2023). This may be due to the slow reactivity of the hemoglobin, the biocatalyst, with the ATRP initiator, or keeping the reaction environment oxygen-free for a week until the polymerization is completed. In this project, cryogels were frozen for seven days. However, longer polymerization time may be needed to achieve higher yields. Insufficient polymerization also leads to a low swelling ratio.

Table 2. Polymerization yield and swelling ratio of Cryogels

	Polymerization yield (%)	Swelling ratio
Cryogels	61.27±3.91	7.46±1.59

Scanning electron microscopy (SEM) illustrated high-resolution images of the internal structure of cryogels, which improved the understanding of microstructure in cryogels, such as pore structures and pore size distribution. The SEM results of cryogels modified by different methods were characterized (**Figure 4, Figure 5**). According to these results, the pore structures resulting from ice crystal melting can be clearly observed. Besides, the difference between **Figure 4** and **Figure 5** is noticeable. **Figure 5** reveals the successful immobilization of a large number of nanoparticles on the cryogels. Based on the scale, **Figure 5d** showed the average diameter of dried nanoparticles was 578 nm, measured by Image J. The difference in the nanoparticle size from the SEM and DLS can be due to the dehydration of the soft nanoparticles during sample preparation for the SEM imaging.

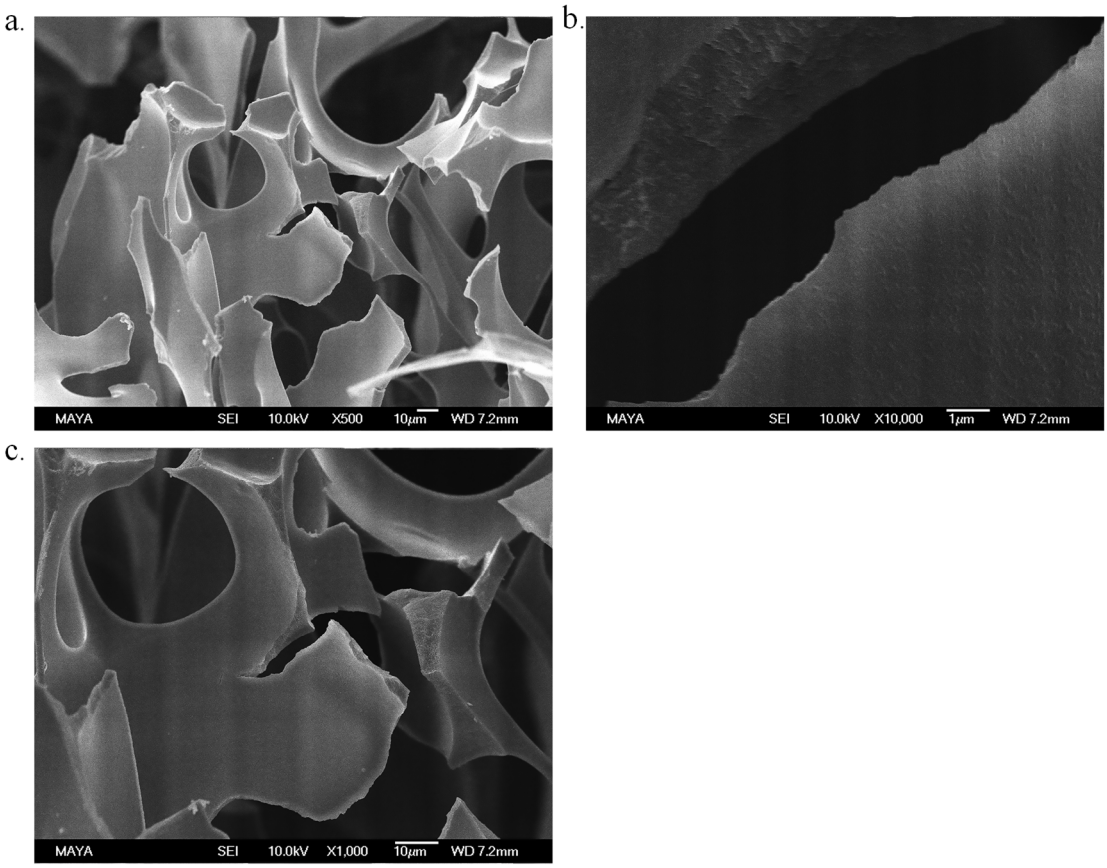

Figure 4. Scanning electron microscopy (SEM) images of cryogels without nanoparticles at different resolutions. a. 500X; b. 1000X; c. 10000X. The scale bars show 10 and 1 μm.

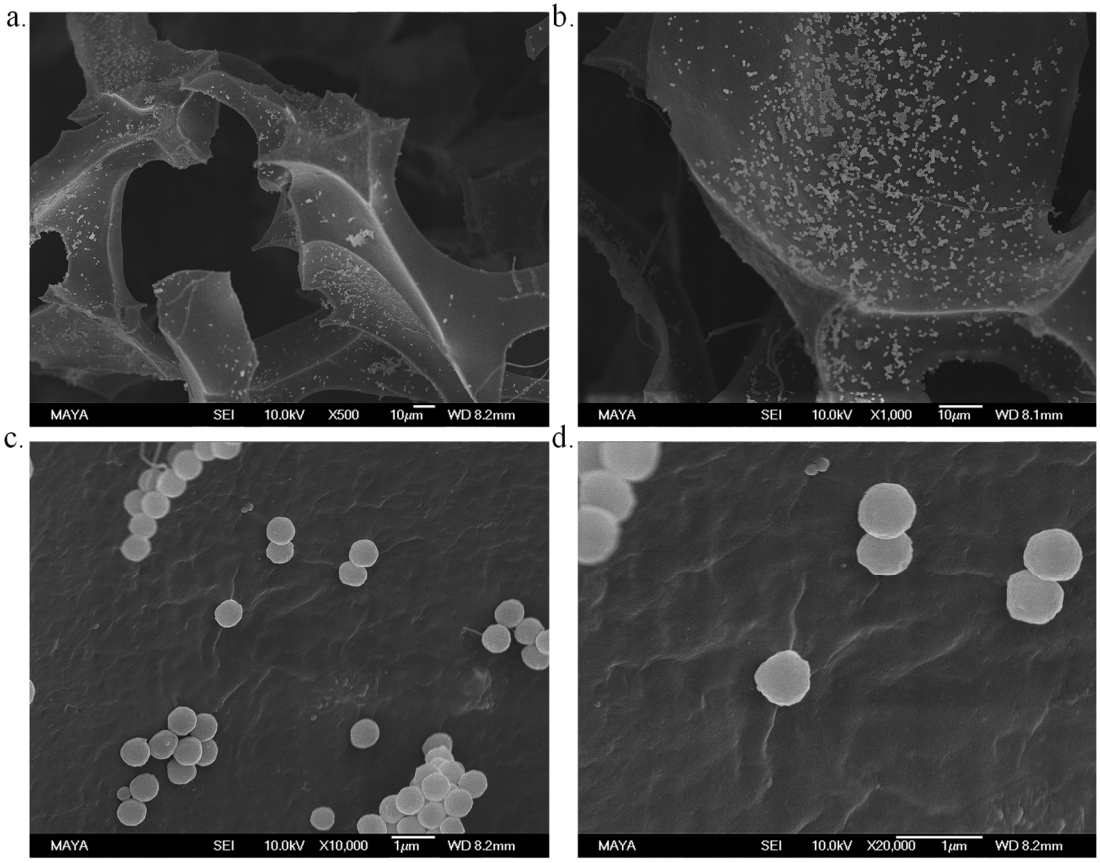

Figure 5. Scanning electron microscopy (SEM) images of cryogels with nanoparticles at different resolutions. a. 500X; b. 1000X; c. 10000X; d. 20000X. The scale bars show 10 and 1 μm.

3.3 Batch Adsorption isotherms

Another critical factor in evaluating cryogels is the capacity and adsorption process. This project conducted batch adsorption and kinetics adsorption for further evaluation. Batch adsorption was used to assess capacity, which can obtain maximum capacity via a suitable model.

The calibration curves for Hemoglobin and Ovalbumin can be seen in **Figures 6** and **7**.

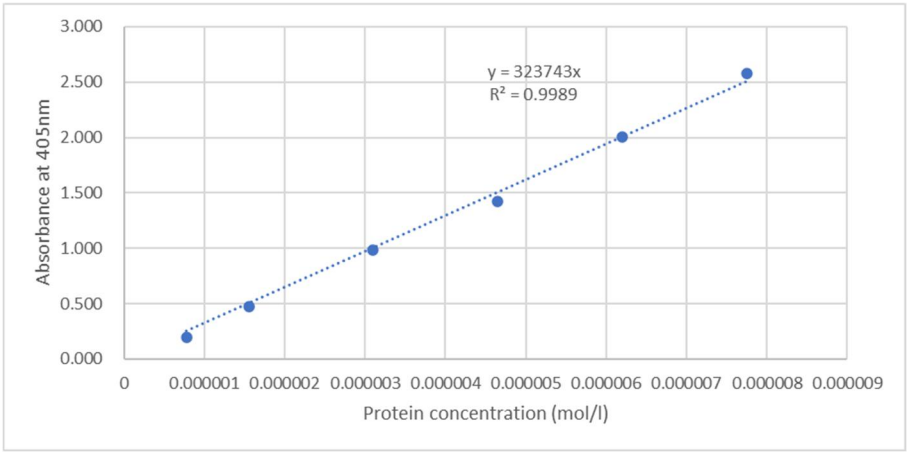

Figure 6. The calibration curve of hemoglobin.

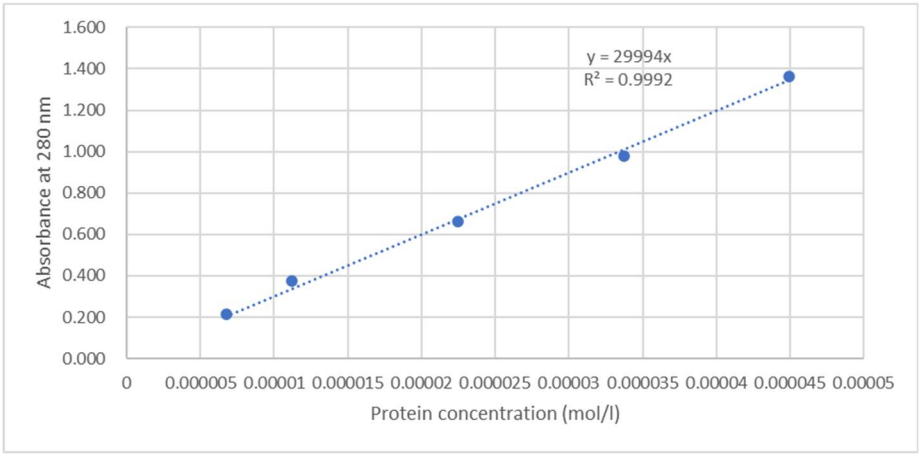

Figure 7. The calibration curve of ovalbumin.

3.3.1 Batch Adsorption of Hemoglobin

The capacity of cryogels was obtained under different protein concentrations via batch adsorption. The adsorption capacity by cryogels in different hemoglobin concentrations is depicted in **Figures 8a** and **8b**. Hemoglobin binds to the cryogels at different angles. Therefore, the binding sites are heterogeneous for MIP since there is no control of how the hemoglobin protein makes its footprint on the surface of the gel. Adsorbate monolayer adsorption onto a homogenous adsorbent surface is simulated for the Langmuir model (Ansell, 2015). Therefore, the simple Langmuir model cannot adequately describe the adsorption situation. The Bis-Langmuir model was selected for fitting to show the adsorption behavior of cryogels and calculated maximum capacity (**Figure 8**), represented as **Equation 3** Where Ce represents the concentration of proteins not adsorbed by cryogels in solution (mg/ml), q_{max1} and q_{max2} are relevant Langmuir constants associated with the adsorption capacity. K_{d1} and K_{d2} are relevant Langmuir constants related to the dissociation constant (Hajizadeh et al., 2018).

$$Q = \frac{C_e \times q_{max1}}{K_{d1} + C_e} + \frac{C_e \times q_{max2}}{K_{d2} + C_e} \qquad \textbf{Equation 3}$$

The maximum capacity can be calculated via **Equation 4**, the value stated in **Table 3**

$$Q_{max} = \frac{weight\ of\ adsorped\ protein\ (mg)}{volume\ of\ cryogels\ (ml)} \qquad \textbf{Equation 4}$$

Based on the results, the maximum capacity of cryogels decreased after the immobilization of nanoparticles. According to **Figure 2** and **Figure 5**, it can be observed that the size of nanoparticles is much larger than that of hemoglobin. Therefore, the nanoparticles covered some of the binding sites on the surface and covered the MIP cavities. Thus, they reduced the Hemoglobin adsorption.

Table 3. The Parameters in Equation 3 and the Maximum Capacity

	q_{max1}	K_{d1}	q_{max2}	K_{d2}	Maximum capacity
Cryogels without nanoparticles	180	0.24	112	0.001	309.70±5.83
Cryogels with nanoparticles	44	0.24	100	0.01	148.58±0.98

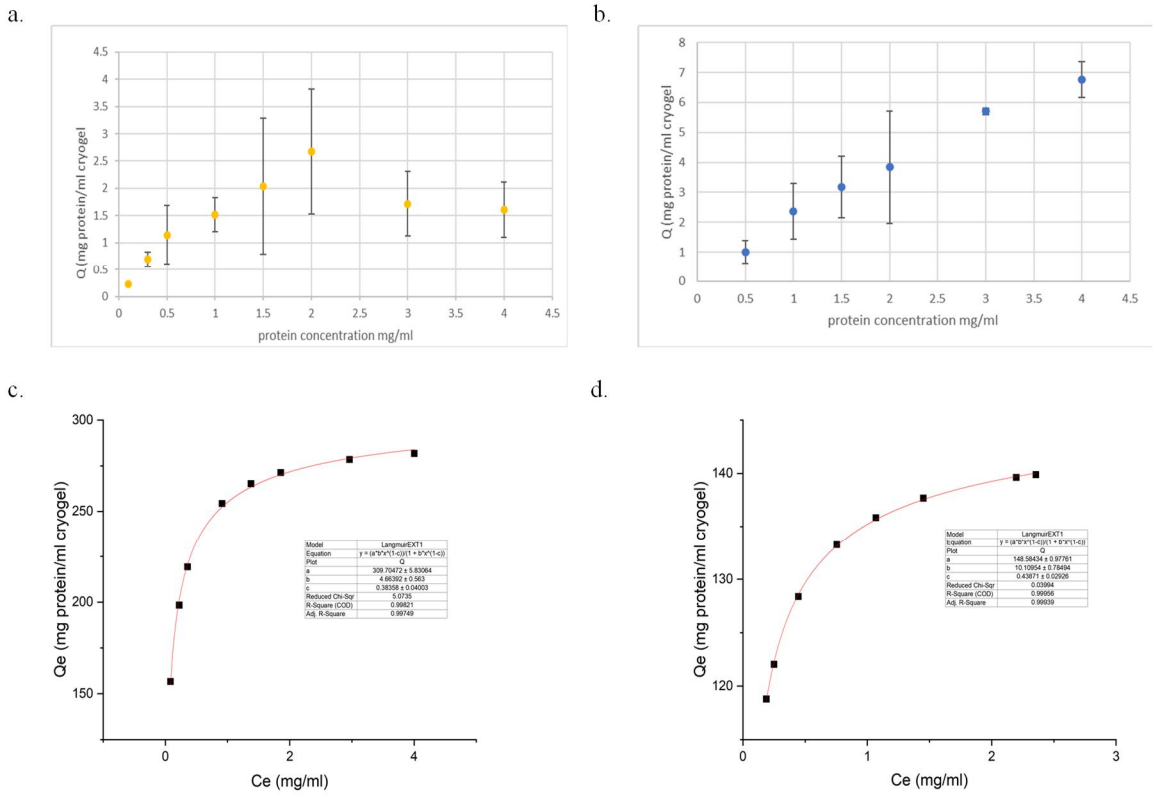

Figure 8. Batch adsorption of hemoglobin. a. The average capacity of cryogels was obtained at different protein concentrations without nanoparticles; b. The average capacity of cryogels was obtained at different protein concentrations with nanoparticles; c. fitting the Bis-Langmuir adsorption isotherm model for hemoglobin adsorption on cryogels without nanoparticles; d. fitting the Bis-Langmuir adsorption isotherm model for hemoglobin adsorption on cryogels with nanoparticles. Ce: The concentration of proteins not adsorbed by cryogels in solution; Qe (Q): The capacity of cryogels was obtained under different protein concentrations.

3.3.2 Batch Adsorption of Ovalbumin

The variation of ovalbumin adsorption capacity by cryogels in different ovalbumin concentrations is depicted in **Figures 9a** and **9b**. Langmuir adsorption isotherm applies to batch adsorption between ConA and ovalbumin (**Equation 5**).

$$Q = \frac{C_e \times q_{max}}{C_e + K_{d1}} \qquad \textbf{Equation 5}$$

Linearized Langmuir adsorption was performed (**Figure 9c, 9d**). Based on **Equation 6**, the maximum capacity can be calculated. The $q_{\max}$ of cryogels without nanoparticles is 43.63 mg protein/ml cryogels; The $q_{\max}$ of cryogels with nanoparticles is 93.98 mg protein/ml cryogels. The increment of maximum capacity indicated nanoparticles concentrated ligands successfully. It further proved the efficiency of glycoprotein purification has been optimized by introducing epoxy group nanoparticles.

$$\frac{1}{Q} = \frac{K_{d1}}{q_{max}} \times \frac{1}{C_e} + \frac{1}{q_{max}} \qquad \textbf{Equation 6}$$

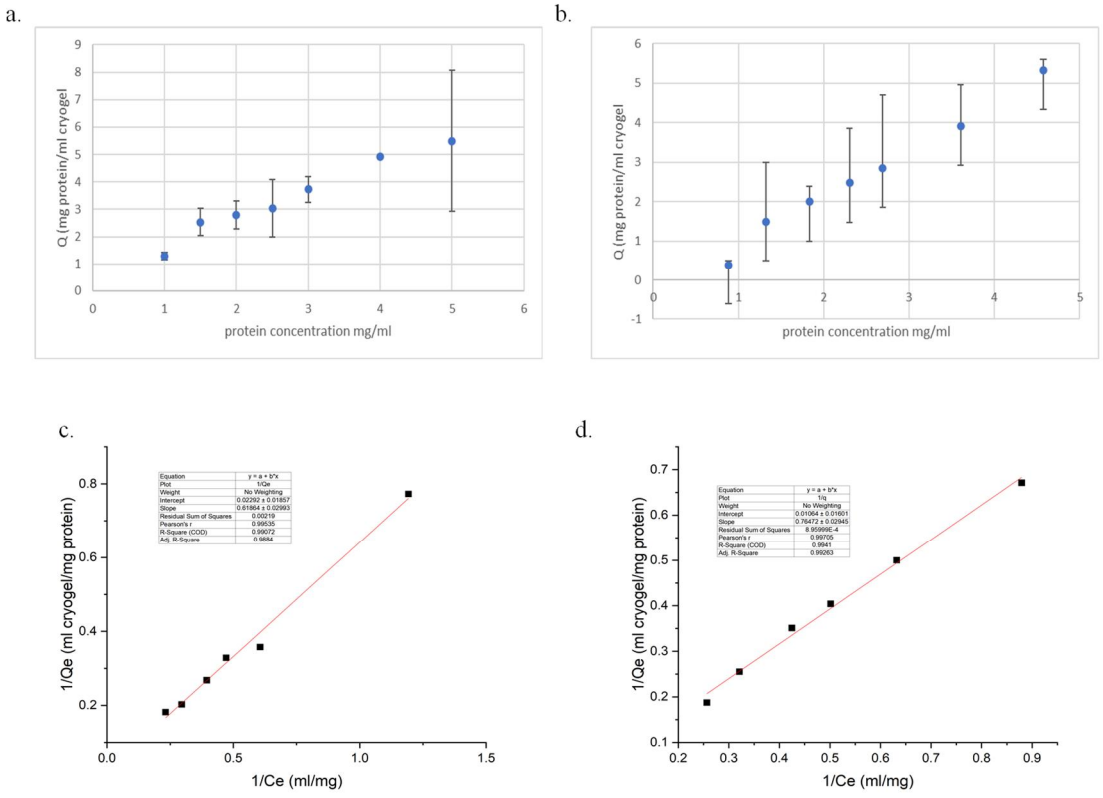

Figure 9. Batch adsorption of ovalbumin. a. The average capacity of cryogels was obtained at different protein concentrations without nanoparticles; b. The average capacity of cryogels was obtained at different protein concentrations with nanoparticles; c. fitting the Langmuir adsorption isotherm model for ovalbumin on cryogels without nanoparticles; d. fitting the Langmuir adsorption isotherm model for ovalbumin on cryogels with nanoparticles. Ce: The concentration

of proteins not adsorbed by cryogels in solution; Qe (Q): The capacity of cryogels obtained under different protein concentrations.

3.4 Kinetics Adsorption isotherms

To express the adsorption process, it is necessary to conduct kinetics adsorption. The pseudo-second-order model is widely used to characterize solute adsorption mechanism in solution. This project used the pseudo-second-order model to fit hemoglobin and ovalbumin adsorption.

3.4.1 Kinetics Adsorption of Hemoglobin

The process of cryogels adsorbing hemoglobin over time is illustrated in **Figure 10**. It can be observed that both types of cryogels reached maximum adsorption capacity at around 4 hours (**Figure 10a,10b**). Linearized pseudo second-order model adsorption was performed (**Figure 10c**, **10d**). Based on **Equation 8**, the maximum can be calculated (Largitte & Pasquier, 2016). The q_{max} of cryogels without nanoparticles is 5.10 mg protein/ml cryogels; The q_{max} of cryogels with nanoparticles is 4.49 mg protein/ml cryogels.

$$Q = \frac{Kq_{max}^2 t}{1+Kq_{max}t} \quad \textbf{Equation 7}$$

$$\frac{t}{Q} = \frac{1}{q_{max}} \times t + \frac{1}{Kq_{max}^2} \quad \textbf{Equation 8}$$

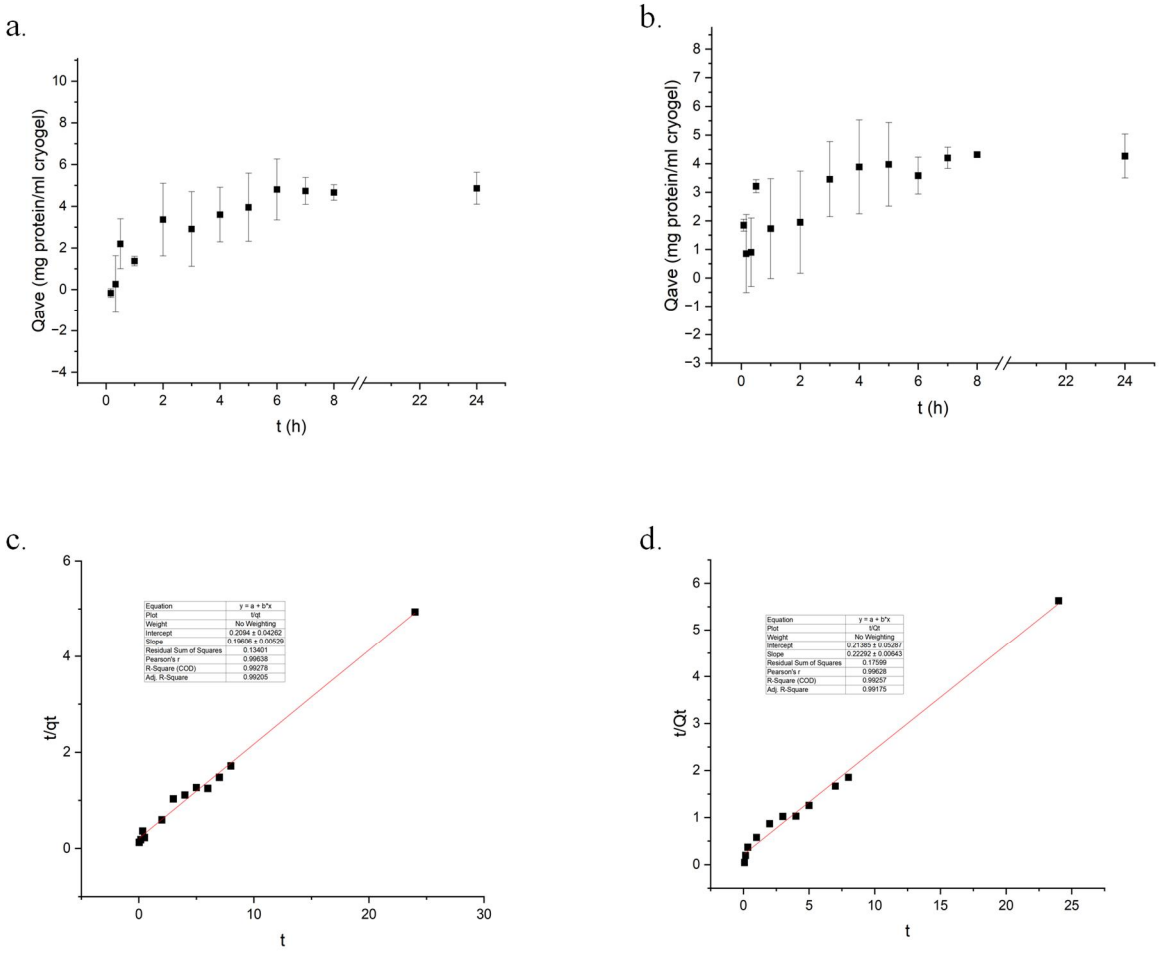

Figure 10. Kinetics Adsorption of Hemoglobin. a. The average capacity of cryogels was obtained at different times without nanoparticles; b. The average capacity of cryogels was obtained at different times with nanoparticles; c. Linearized Pseudo second-order model of hemoglobin on cryogels without nanoparticles; d. Linearized Pseudo second-order model of hemoglobin on cryogels with nanoparticles; t: time; Qt(qt/Qave): The capacity of cryogels obtained under different times.

3.4.2 Kinetics Adsorption of Ovalbumin

The process of cryogels adsorbing ovalbumin over time is illustrated in **Figure 11**. It can be observed that cryogels without nanoparticles reached maximum adsorption capacity at around 2 hours. However, the cryogels with nanoparticles reached maximum adsorption capacity at around 6 hours (**Figure 11a,11b**). The time to reach maximum adsorption capacity lengthened after the immobilization of nanoparticles. The pseudo-second-order model was also applied in ovalbumin kinetics adsorption. Based on **Equation 8**, the maximum capacity can be calculated. The q_{max} of cryogels without nanoparticles is 6.09 mg protein/ml cryogels; The q_{max} of cryogels with nanoparticles is 12.75 mg protein/ml cryogels.

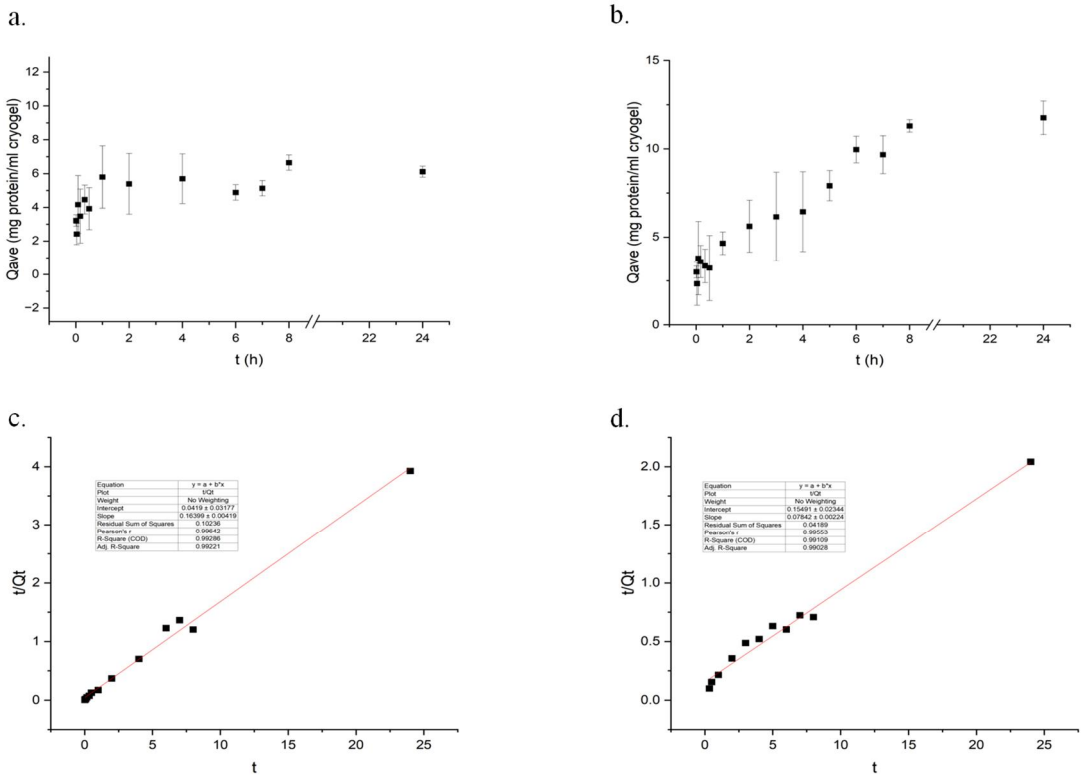

Figure 11. Kinetics Adsorption of Ovalbumin. a. The average capacity of cryogels was obtained at different times without nanoparticles; b. The average capacity of cryogels was obtained at different times with nanoparticles; c. Linearized Pseudo second-order model of ovalbumin on cryogels without nanoparticles; d. Linearized Pseudo second-order model of ovalbumin on cryogels with nanoparticles; t: time; Qt(qt/Qave): The capacity of cryogels obtained under different times.

Compared to batch adsorption, the maximum capacity of hemoglobin and ovalbumin decreased significantly. Here are some possible reasons; Due to the presence of ligands, this project applied mild regeneration conditions to avoid damaging Con A. Thus, the regeneration did not remove all hemoglobin each time. As the number of regenerations increased, capacity decreased. Besides, each model makes different assumptions about the adsorption behavior, leading to the difference in ultimately calculated maximum capacity.

3.5 Selective adsorption characterization of cryogels

The SDS-PAGE was used to evaluate the specific adsorption of hemoglobin in cryogels. This section loaded the 6 mg/ml bovine serum albumin (BSA) and 3 mg/ml hemoglobin mixture solution in cryogels with nanoparticles. Use SDS-PAGE to analyze loaded, washed, and eluted fractions, which characterize the selective adsorption of hemoglobin (**Figure 12**). The molecular weight of BSA is 66 kDa, which characterized the band of SDS-PAGE in 66 kDa. Hemoglobin, as a hetero-tetramer, showed multiple bands in SDS-PAGE. The molecular weight of each subunit is 16 kDa. Thus, SDS-PAGE analysis of hemoglobin bands can be characterized as monomers (16 kDa), dimers (32 kDa), trimers (48 kDa), and tetramers (64 kDa) in lane 3 of **Figure 12** (Russo et al., 2013). Based on the

results, it can be observed that washed fractions contain a large number of BSA. In eluted fractions, the tetramers and monomers of hemoglobin can be observed. Based on the selection of the protein, it is difficult to draw firm conclusions about selectivity. The hemoglobin tetramer and BSA have very close bands (64 and 66 KDa, respectively). Additional experiments are required to confirm the band around 60 KDa, belongs to which protein. The other hypothesis is that BSA protein is also attached to the cryogel. The pH of binding buffer is 6.8. Cryogels are positively charged and BSA is negatively charged. Thus, BSA protein attached to cryogels possiblely. What is clear from the SDS-PAGE is that the other impurities present in BSA and hemoglobin solution do not bind to the column.

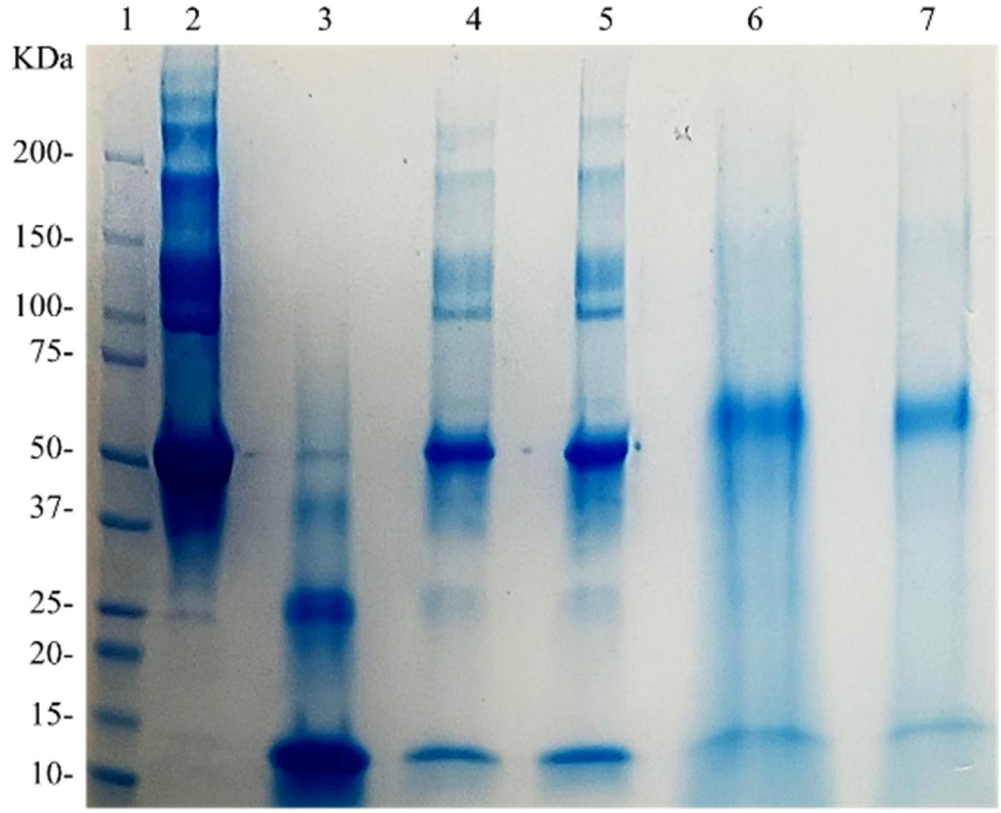

Figure 12. Digital image of SDS-PAGE results. Lane: 1. Marker; 2. BSA solution (6mg/ml); 3. Hemoglobin (3mg/ml); 4. Washed fractions from cryogels; 5. loaded fractions on cryogels; 6 eluted fractions on cryogels; 7. Diluted eluted fractions on cryogels.

Conclusion

In this project, hemoglobin is verified as a biocatalyst to synthesize cryogels under the ATRPase. The resulting multifunctional cryogels demonstrated successful purification of hemoglobin and ovalbumin. The purification of ovalbumin was optimized effectively by introducing epoxy group nanoparticles. The maximum adsorption capacity of ovalbumin doubled after immobilized nanoparticles. However, nanoparticles occupied some bind sites of hemoglobin on the surface of cryogels. The maximum adsorption capacity of hemoglobin decreased in cryogels with nanoparticles. Meanwhile, cryogels still have exceptional selective adsorption to hemoglobin. Therefore, the multifunctional cryogels can purify multiple proteins simultaneously and efficiently. This shows the potential of cryogels as successful multifunctional stationary phases in chromatography.

In the future, the synthesis conditions for cryogels using hemoglobin as a biocatalyst can be optimized to improve the polymerization yield and stability of the cryogels, such as extending the time for polymerization or removing oxygen more thoroughly. Besides, only batch adsorption was conducted for this project. The continuous mode is more suitable for assessing the chromatography procedure than the batch mode. Thus, subsequent work should consider implementing continuous adsorption to achieve greater capacity. Additionally, improving the scale and types of purified protein is essential, which makes multifunctional chromatography more applicable.

Reference

Ansell, R. J. (2015). Characterization of the binding properties of molecularly imprinted polymers. In Advances in biochemical engineering, biotechnology (pp. 51–93). https://doi.org/10.1007/10_2015_316

Baimenov, A., Berillo, D., Poulopoulos, S. G., & Inglezakis, V. J. (2020). A review of cryogels synthesis, characterization and applications on the removal of heavy metals from aqueous solutions. Advances in Colloid and Interface Science, 276, 102088. https://doi.org/10.1016/j.cis.2019.102088

Bercea, M., & Lupu, A. (2024). Recent Insights into Glucose-Responsive Concanavalin A-Based Smart Hydrogels for Controlled Insulin Delivery. Gels, 10(4), 260. https://doi.org/10.3390/gels10040260

Beyazit, S., Bui, B. T. S., Haupt, K., & Gonzato, C. (2016). Molecularly imprinted polymer nanomaterials and nanocomposites by controlled/living radical polymerization. Progress in Polymer Science, 62, 1–21. https://doi.org/10.1016/j.progpolymsci.2016.04.001

Chen, L., Wang, X., Lü, W., Wu, X., & Li, J. (2016). Molecular imprinting: perspectives and applications. Chemical Society Reviews, 45(8), 2137–2211. https://doi.org/10.1039/c6cs00061d

Coessens, V., Pintauer, T., & Matyjaszewski, K. (2001). Functional polymers by atom transfer radical polymerization. Progress in Polymer Science, 26(3), 337–377. https://doi.org/10.1016/s0079-6700(01)00003-x

Coşkun, Ö. (2016). Separation tecniques: CHROMATOGRAPHY. İstanbul Kuzey Klinikleri. https://doi.org/10.14744/nci.2016.32757

Gao, S., Song, W., & Guo, M. (2020). The integral role of bioproducts in the growing bioeconomy. Industrial Biotechnology, 16(1), 13–25. https://doi.org/10.1089/ind.2019.0033

González, M. G., Cabanelas, J. C., & Baselga, J. (2012). Applications of FTIR on epoxy resins - identification, monitoring the curing process, phase separation and water uptake. In InTech eBooks. https://doi.org/10.5772/36323

Gottschalk, U. (2008). Bioseparation in antibody manufacturing: the good, the bad and the ugly. Biotechnology Progress, 24(3), 496–503. https://doi.org/10.1021/bp070452g

Hajizadeh, S., Kettisen, K., Gram, M., Bülow, L., & Ye, L. (2018). Composite imprinted macroporous hydrogels for haemoglobin purification from cell homogenate. Journal of Chromatography a/Journal of Chromatography, 1534, 22–31. https://doi.org/10.1016/j.chroma.2017.12.038

Hajizadeh, S., Kirsebom, H., Leistner, A., & Mattìasson, B. (2012). Composite cryogel with immobilized concanavalin A for affinity chromatography of glycoproteins. Journal of Separation Science, 35(21), 2978–2985. https://doi.org/10.1002/jssc.201200433

Hajizadeh, S., Mattiasson, B., & Kirsebom, H. (2013). Flow‐Through‐Mediated surface immobilization of Sub‐Micrometre particles in monolithic cryogels. *Macromolecular Materials and Engineering*, *299*(5), 631–638. https://doi.org/10.1002/mame.201300358

Hajizadeh, S., Mattìasson, B., & Kirsebom, H. (2013c). Flow-Through-Mediated surface immobilization of Sub-Micrometre particles in monolithic cryogels. Macromolecular Materials and Engineering, 299(5), 631–638. https://doi.org/10.1002/mame.201300358

He, S., Zhang, L., Bai, S., Yang, H., Cui, Z., Zhang, X., & Li, Y. (2021). Advances of molecularly imprinted polymers (MIP) and the application in drug delivery. European Polymer Journal/European Polymer Journal, 143, 110179. https://doi.org/10.1016/j.eurpolymj.2020.110179

Kali, G., Silva, T. B., Sigg, S. J., Seidi, F., Renggli, K., & Bruns, N. (2012). ATRPAses: Using nature's catalysts in atom transfer radical polymerizations. In ACS symposium series (pp. 171–181). https://doi.org/10.1021/bk-2012-1100.ch011

Largitte, L., & Pasquier, R. (2016). A review of the kinetics adsorption models and their application to the adsorption of lead by an activated carbon. Process Safety and Environmental Protection/Transactions of the Institution of Chemical Engineers. Part B, Process Safety and Environmental Protection/Chemical Engineering Research and Design/Chemical Engineering Research & Design, 109, 495–504. https://doi.org/10.1016/j.cherd.2016.02.006

Matyjaszewski, K., & Xia, J. (2001). Atom Transfer radical polymerization. Chemical Reviews, 101(9), 2921–2990. https://doi.org/10.1021/cr940534g

Memić, A., Colombani, T., Eggermont, L. J., Rezaeeyazdi, M., Steingold, J. M., Rogers, Z. J., Joshi-Navare, K., Mohammed, H. S., & Bencherif, S. A. (2019). Latest advances in Cryogel technology for biomedical applications. Advanced Therapeutics, 2(4). https://doi.org/10.1002/adtp.201800114

Patel, H. (2021). Comparison of batch and fixed bed column adsorption: a critical review. International Journal of Environmental Science and Technology, 19(10), 10409–10426. https://doi.org/10.1007/s13762-021-03492-y

Prasad, K. K., & Prasad, N. K. (2010). Downstream Process Technology: A New Horizon In Biotechnology. PHI Learning Pvt. Ltd.

Russo, R., Zucchelli, S., Codrich, M., Marcuzzi, F., Verde, C., & Gustincich, S. (2013). Hemoglobin is present as a canonical α2β2 tetramer in dopaminergic neurons. Biochimica Et Biophysica Acta. Proteins and Proteomics, 1834(9), 1939–1943. https://doi.org/10.1016/j.bbapap.2013.05.005

Saleemuddin, M., & Husain, Q. (1991). Concanavalin A: A useful ligand for glycoenzyme immobilization—A review. Enzyme and Microbial Technology, 13(4), 290–295. https://doi.org/10.1016/0141-0229(91)90146-2

Silva, T. B., Spulber, M., Kocik, M. K., Seidi, F., Charan, H., Rother, M., Sigg, S. J., Renggli, K., Kali, G., & Bruns, N. (2013). Hemoglobin and red blood cells catalyze atom transfer radical polymerization. Biomacromolecules, 14(8), 2703–2712. https://doi.org/10.1021/bm400556x

Solmaz, S. H. (2023). Application of composite cryogels in downstream processing - A review. Reactive and Functional Polymers/Reactive & Functional Polymers, 191, 105693. https://doi.org/10.1016/j.reactfunctpolym.2023.105693

Surolia, A., Bishayee, S., Ahmad, A., Balasubramanian, K., Thambi-Dorai, D., Podder, S., & Bachhawat, B. K. (1975). Studies on the Interaction of Concanavalin A with Glycoproteins. In Advances in experimental medicine and biology (pp. 95–115). https://doi.org/10.1007/978-1-4684-0949-9_6

Trinh, T. H. T., Ye, L., & Hajizadeh, S. (2023). Impact of double cryogelation process on a macroporous dye-affinity hydrogel. Journal of Separation Science, 46(8). https://doi.org/10.1002/jssc.202300017

Wurm, F. M. (2004). Production of recombinant protein therapeutics in cultivated mammalian cells. Nature Biotechnology, 22(11), 1393–1398. https://doi.org/10.1038/nbt1026

Zhang, T., Wang, S., Lu, X., Guo, Y., & Liang, X. (2023). A composite hydrogel modified silica stationary phase for mixed mode liquid chromatography. Journal of Chromatography a/Journal of Chromatography, 1707, 464300. https://doi.org/10.1016/j.chroma.2023.464300

Appendix

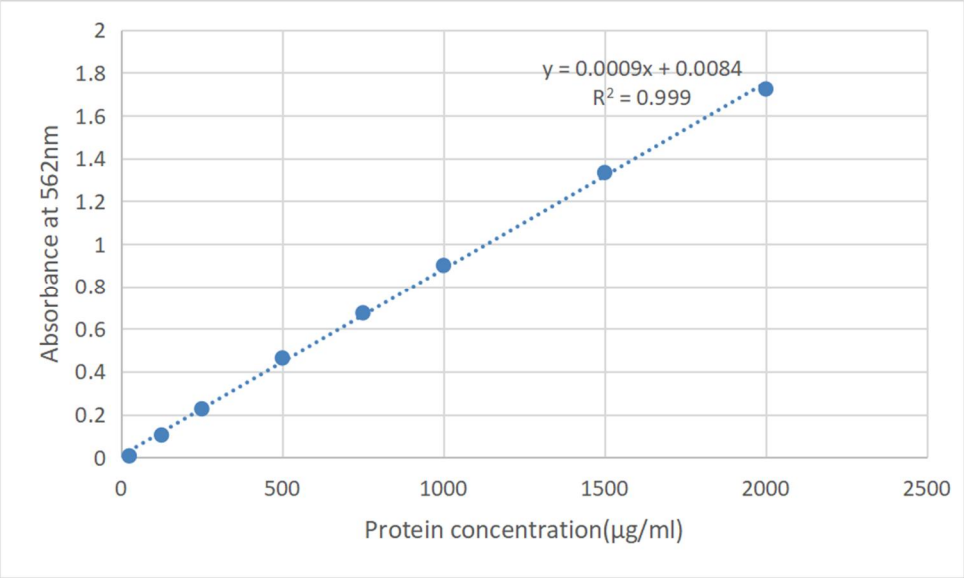

Figure S1. The calibration curve of albumin to calculate the concentration of unbound concanavalin A.